

# Gravitational waves from in-spirals of compact objects in binary common-envelope evolution

Yonadav Barry Ginat,<sup>1\*</sup> Hila Glanz,<sup>1</sup> Hagai B. Perets,<sup>1</sup> Evgeni Grishin<sup>1</sup> and Vincent Desjacques<sup>1</sup>

<sup>1</sup>*Faculty of Physics, Technion – Israel Institute of Technology, Haifa, 3200003, Israel*

Accepted XXX. Received YYY; in original form ZZZ

## ABSTRACT

Detection of gravitational-wave (GW) sources enables the characterisation of binary compact objects and of their in-spiral. However, other dissipative processes can affect the in-spiral. Here we show that the in-spiral of compact objects through a gaseous common-envelope (CE) arising from an evolved stellar companion produces a novel type of GW-sources, whose evolution is dominated by the dissipative gas dynamical friction effects from the CE, rather than the GW-emission itself. The evolution and properties of the GW-signals differ from those of isolated gas-poor mergers significantly. We find characteristic strains of  $\sim 10^{-23}$ – $10^{-21}$  ( $10\text{kpc}/D$ ) for such sources – observable by next-generation space-based GW-detectors. The evolution of the GW-signal can serve as a probe of the interior regions of the evolved star, and the final stages of CE-evolution, otherwise inaccessible through other observational means. Moreover, such CE-mergers are frequently followed by observable explosive electromagnetic counterparts and/or the formation of exotic stars.

**Key words:** Gravitational waves — (stars:) binaries (including multiple): close

## 1 INTRODUCTION

Two gravitating bodies emit gravitational waves (GWs) when orbiting each other, whose amplitude and frequency depend on their relative acceleration, which, in turn, depends on their masses and separation. Generally, larger masses and smaller separations induce stronger accelerations and stronger GW emission. Current and upcoming GW-detectors cannot detect mergers of stellar binaries, whose radii – and separation at merger – are far below the amplitude sensitivity of the detectors at the relevant frequencies. Indeed, only sufficiently compact (and massive) stars could serve as detectable GW sources; current studies typically focus on the mergers of white dwarfs (WDs) (Amaro-Seoane et al. 2017), neutron stars (NSs), and black holes (BHs) (Abbott et al. 2016b, 2018). However, the stellar cores of evolved stars could serve as a novel type of compact object (CO) to produce GW sources, once they merge with another compact object. Such mergers can occur following a binary common-envelope (CE) evolution of evolved stars with compact companions, leading to the in-spiral of the companion and to its merger with the core of the evolved star (Ivanova et al. 2013).

During the evolution of stars beyond their main-

sequence evolutionary stage, they fuse the hydrogen in their cores into helium and heavier elements, that accumulate in compact cores. The stellar envelopes of the stars then expand to large radii – tens, or even up to hundreds of solar radii (during the red-giant branch, and asymptotic giant branch, phases of their evolution, as well as the Wolf-Rayet stage for very massive stars). When such an evolved star has a close stellar companion the expanded envelope engulfs the companion and, under appropriate conditions, creates a shared envelope of gas, covering both the core of the evolved star and the companion (Ivanova et al. 2013). The stellar companion is then thought to spiral inside the envelope due to its gravitational interaction with the gas (see figure 1 for depictions of such in-spirals). The CE phase could result in either an ejection of the gaseous envelope before the companion arrives at the core, or in a final merging of the companion with the compact core. The former occurs when the evolved stellar envelope is not sufficiently massive and dense compared with the stellar companion, and *vice versa*. Here we show that when the stellar companion is compact, and the core is also sufficiently compact, CE evolution leads to various possible CO-core mergers with detectable GW signals (see Nazin & Postnov 1995, 1997 for an initial study for neutron star companions). Note that significant fractions of the envelope may be ejected on much longer non-dynamical

\* E-mail: ginat@campus.technion.ac.il

timescales (Glanz & Perets 2018; Michaely & Perets 2019); this, however is always preceded by the dynamical phase.

The in-spiral of a compact object proceeds on a dynamical timescale when the dynamical friction due to the CE is sufficiently strong. The closest approach accessible for a CO-core binary occurs when the CO reaches the tidal radius of the core  $r_t \sim (M_{\text{CO}}/M_{\text{core}})^{1/3} R_{\text{core}}$ , at which point the latter is disrupted tidally. To characterise the GW-detectability of such binary mergers, one needs to derive the strain and frequency of the GW emission of such binaries close to the final radius. One also needs to account for the evolution due to the interaction with the gaseous envelope. This process is special, in-so-far as the driving force behind the in-spiral is not energy-loss to gravitational waves, but rather interaction with an environment. As such the gravitational-wave signal should reflect the properties of the environment, and allow for potentially direct observations of such otherwise-inaccessible environments/processes (Pani 2015; Fedrow et al. 2017).

To study such GW sources we model the evolution as two point masses orbiting inside an envelope with a given constant density profile, and we neglect the back-reaction of the motion of the system on the envelope itself. We model the in-spiral through the effects of gas dynamical friction (GDF) using an approach originally presented by Ostriker (1999), rather than the approach taken previously by Nazin & Postnov (1995), and include 2.5 post-Newtonian corrections to the gravitational interaction of the CO and the core. The resultant GW signal would depend on the density profile of the CE, thereby enabling the utilization of gravitational waves to probe the properties of the interior of the red-giant/CE.

The in-spiral is driven by GDF and not by aerodynamic drag, due to the high ratio between the mass of the in-spiralling CO and its geometric cross-section. Grishin & Perets (2015) found that the critical transition radius between GDF-dominated evolution and aerodynamic-drag dominated evolution is  $R_c \propto v_{\text{rel}}/\sqrt{G\rho_m}$ , where  $v_{\text{rel}}$  is the relative velocity between the CO and the gas, and  $\rho_m$  is the density of the CO. The proportionality constant depends on the dimensionless Reynolds and Mach numbers of the flow, and is of order unity for most plausible situations.

In our case, we take an initial relative velocity of  $\sim 100 \text{ km s}^{-1}$  (similar to the Keplerian velocity around a massive star at 1 AU). For a typical WD density of  $\rho_{\text{WD}} \approx 10^6 \text{ g cm}^{-3}$ , we get a critical radius of a few percent of the WD radius,  $R_c \approx 0.05 R_{\text{WD}}$ , with  $R_{\text{WD}} = 0.01 R_{\odot}$ . For typical NS densities of  $\rho_{\text{NS}} = 10^{14} \text{ g cm}^{-3}$ , the critical radius is around  $4 \times 10^3 \text{ cm}$ , much less than a NS radius. Therefore, for compact objects embedded in envelopes of giant stars, GDF dominates over aerodynamic drag.

We begin by describing the set-up of our models and the equations of motion, which we numerically integrate to calculate the GW signatures of the CE gravitational-wave (CEGW) sources, exploring various configurations of CE-binaries and COs. We then discuss the properties of such CEGW sources and the possibility of detecting them, and then we summarise.

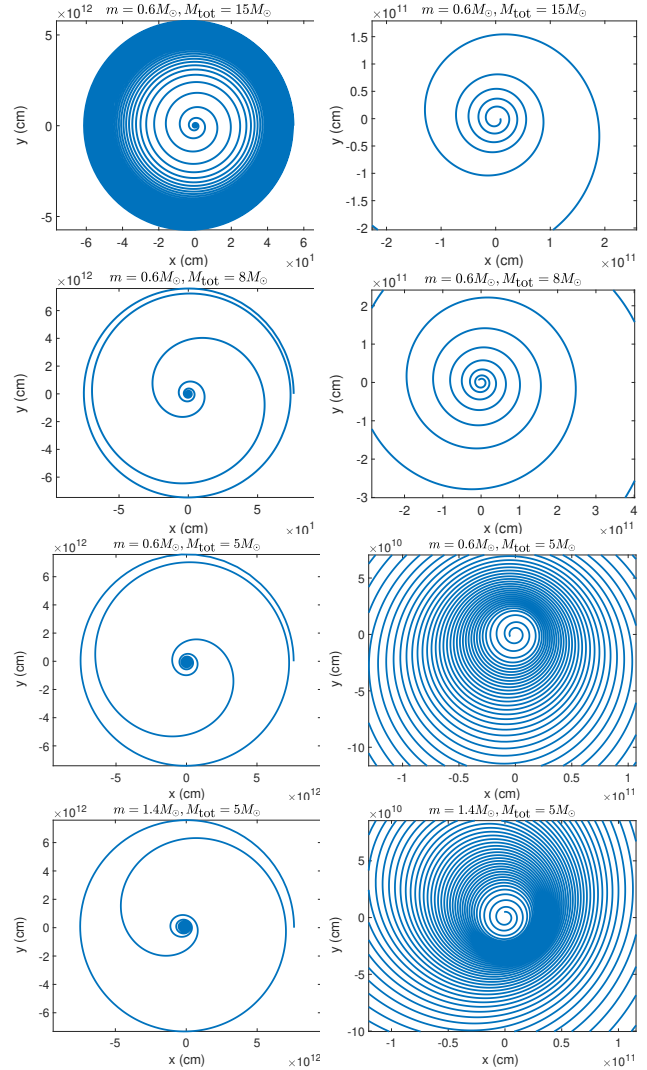


**Figure 1.** The separation between the companion and the core, for the some of the different mass combinations described in the text. Each combination is displayed twice, with the second panel focussing on the central region.

## 2 MODEL DESCRIPTION

We work in the centre-of-mass frame of the binary, and neglect any back-reaction of the companion on the envelope – we take the density of the envelope to be constant in time, and ‘glued’ to the core of the star, which we model as a point mass<sup>1</sup>. This system may be described as an effective one body, whose position  $\mathbf{r}$  describes the relative separation between the companion and the core. Its equations of motion are

$$\ddot{\mathbf{r}} = -\frac{G(M+m)}{r^3}\mathbf{r} - \frac{GM_{\text{env}}(r)}{r^3}\mathbf{r} - F(\mathbf{r}, \mathbf{v})\mathbf{v} + \text{P.N.}, \quad (1)$$

where  $M_{\text{env}}(r)$  is the mass of the envelope inside a sphere of radius  $r$  (excluding the core),  $M = M_{\text{core}}$  is the core

<sup>1</sup> This approximation is more consistent for cases where the envelope is significantly more massive than the companion (see below). In practice, the CE evolution changes the structure of the envelope even when the envelope is more massive.

mass, and  $m = M_{\text{CO}}$  is the companion mass, and ‘P.N.’ denotes post-Newtonian terms. We further define  $M_{\text{tot}} = M + M_{\text{env}}(R)$ , where  $R$  is the radius of the envelope.  $F$  describes the effects due to GDF, which model like [Ostriker \(1999\)](#):

$$F(\mathbf{r}, \mathbf{v}) = \frac{2\pi G^2 m \rho(\mathbf{r})}{v^3} \begin{cases} \ln \left( \frac{1+\mathcal{M}}{1-\mathcal{M}} e^{-2\mathcal{M}} \right), & \mathcal{M} < 1 \\ \ln \left( \Lambda^2 - \frac{\Lambda^2}{\mathcal{M}^2} \right), & \mathcal{M} > 1. \end{cases} \quad (2)$$

where  $\mathcal{M} = v/c_s$  is the Mach number, and  $c_s$  is the local sound-speed of the envelope. The Coulomb logarithm  $\ln \Lambda$  is given by  $\Lambda = b_{\text{max}}/b_{\text{min}}$  ([Binney & Tremaine 2008](#), p. 835), where  $b_{\text{min}} = \max \{Gm/v^2, r_{\text{coll}}\}$ ;  $r_{\text{coll}}$  is the radius at which the compact object collides with the core. We take  $b_{\text{max}} = 2r$ , as in [Kim & Kim \(2007\)](#) rather than  $b_{\text{max}} = R_{\text{env}}$ , because the density outside  $r$  is a lot smaller than the density inside  $r$ .

### 2.1 Time-Scales

During the most of the in-spiral  $v > c_s$ , and the dynamical friction force is well approximated by

$$F(\mathbf{r}, \mathbf{v}) \sim N \frac{G^2 m^2 \rho(r)}{v^3}, \quad (3)$$

where  $N$  is a dimensionless constant, proportional to the Coulomb logarithm  $\ln \Lambda$ . Let us try to get an order-of-magnitude estimate on the decay time: as  $F_{DF} = -Fv \sim v^{-2}$ , we can treat the orbit as approximately circular. Taking  $v^2 \sim G(M+m+M_{\text{env}}(r))/r$ , gives a collapse time-scale of

$$\tau_{DF} = \frac{\mu v^3}{N G^2 m^2 \bar{\rho}} \sim \frac{\mu(M+m+M_{\text{env}}(r))^{3/2}}{N r^{3/2} \sqrt{G} m^2 \bar{\rho}}. \quad (4)$$

If we take  $\rho = \bar{\rho}$ , we need to take  $r$  as the radius at which the density is equal to the average density, which we denote by  $r = CR$ , where  $C < 1$  describes the concentration of the system. Setting  $M_{\text{env}}(r) \approx M_{\text{env}}$ , we have

$$\begin{aligned} \tau_{DF} &= \frac{4\pi\mu(M+m+M_{\text{env}})^{3/2}a^{3/2}}{3C^{3/2}N\sqrt{G}m^2M_{\text{env}}} \\ &= 0.1 \text{ year} \left( \frac{M+m+M_{\text{env}}}{2M_{\odot}} \right)^{3/2} \left( \frac{R}{100R_{\odot}} \right)^{3/2} \\ &\times \left( \frac{M_{\odot}}{m} \right)^2 \left( \frac{M_{\odot}}{M_{\text{env}}} \right) \left( \frac{0.1}{C} \right)^{3/2} \left( \frac{4 \ln 10}{N} \right). \end{aligned} \quad (5)$$

### 2.2 Wave-Forms

During the in-spiral the binary emits gravitational waves due to a changing quadrupole moment. As  $r$  decreases, the orbital acceleration increases, and so does the GW-amplitude, right up to the final merger. The leading-order GW-strain  $h_{ab}(t)$  is given by the quadrupole formula:

$$h_{ab}^{TT}(t) = \frac{2G}{Dc^4} \ddot{Q}_{ab}^{TT}(t_{\text{ret}}), \quad (6)$$

where  $TT$  denotes the transverse-traceless gauge, and an upper  $TT$  on  $Q$  implies a projection on the direction of observation;  $Q_{ab} = M^{ab} - \delta_{ab}M^{kk}/3$  is the quadrupole moment, and  $t_{\text{ret}} = t - D/c$  is the retarded time, with  $D$  being source-to-detector distance. Even though one of the bodies is not

point-like, it is spherical, so the mass moment is

$$M^{ij} = m x_1^i(t) x_1^j(t) + M_{\text{tot}} x_2^i(t) x_2^j(t) + \frac{1}{3} \delta^{ij} C, \quad (7)$$

where  $C$  is a higher moment of the density  $\rho$ , and  $\mathbf{x}_{1,2}$  is the position of the centre of the CO/giant. The second term does not contribute to  $Q_{ab}$ , so we can ignore it. The contribution of the evolved star is thus equal to that of a point mass, and we may therefore use the formula for  $M^{ij}$  of a binary system in the centre-of-mass frame (e.g. given by equation (3.72) of [Maggiore 2008](#)). The solution to equation (1) defines the wave-form, so the problem of calculating the wave-form reduces to solving the equations of motion.

## 3 NUMERICAL CALCULATIONS

To calculate the CEGW signatures, we integrate equation (1) numerically using a Runge-Kutta integrator (MATLAB’s ode113). We added relativistic corrections to the motion of the core and the companion up to 2.5PN (to account for GW dissipation)<sup>2</sup>, as given by [Lincoln & Will \(1990\)](#). The orbit can still be described by a point particle with mass  $\mu = mM_{\text{tot}}/(m+M_{\text{tot}})$ , moving under the influence of the gravitational field a mass  $M+m$  and inside the envelope’s potential. Here we considered a few combinations of  $m, M$  and  $M_{\text{env}}$  (see table 1 and figure 1).

The density profiles of the stars were obtained from stellar evolution models, produced by the MESA code ([Paxton et al. 2011, 2013, 2015](#)), evolved from initial masses of 15, 8 and 5  $M_{\odot}$ , until they reached  $110R_{\odot}$ ; the stars retained almost all of their original mass. Examples of orbits are shown in figure 1.

For each of these models we calculate the emitted waves, with  $m = 0.6M_{\odot}$  representing a WD companion, and  $m = 1.4M_{\odot}$  – a NS. The detector is assumed to be at a distance of 10 kpc. The resulting wave-forms are shown in figure 2. All in-spirals show a characteristic evolution beginning with regular low-amplitude oscillations at the early phases, which then gradually increase in frequency and amplitude down to the final plunge accompanied by a high amplitude burst.

## 4 DETECTABILITY

Let us proceed to consider the detectability of such CEGWs: the size of the core is comparable to (or larger than) that of WDs, and the orbital frequency of the binary before its final merger is therefore lower than the detection range of aLIGO. However, as we show below, such GW sources are detectable by next-generation space-based GW-detectors, such as LISA.

Whether the predicted signal is detected or not is determined by its characteristic strain, which is related to the signal-to-noise ratio (SNR). If  $S_n(f)$  is the noise power-spectrum density of a detector, and  $h$  is the signal (without

<sup>2</sup> These have significant contributions only when they are extremely close to each other, so the post-Newtonian terms do not include the gravity of the gas in the envelope.

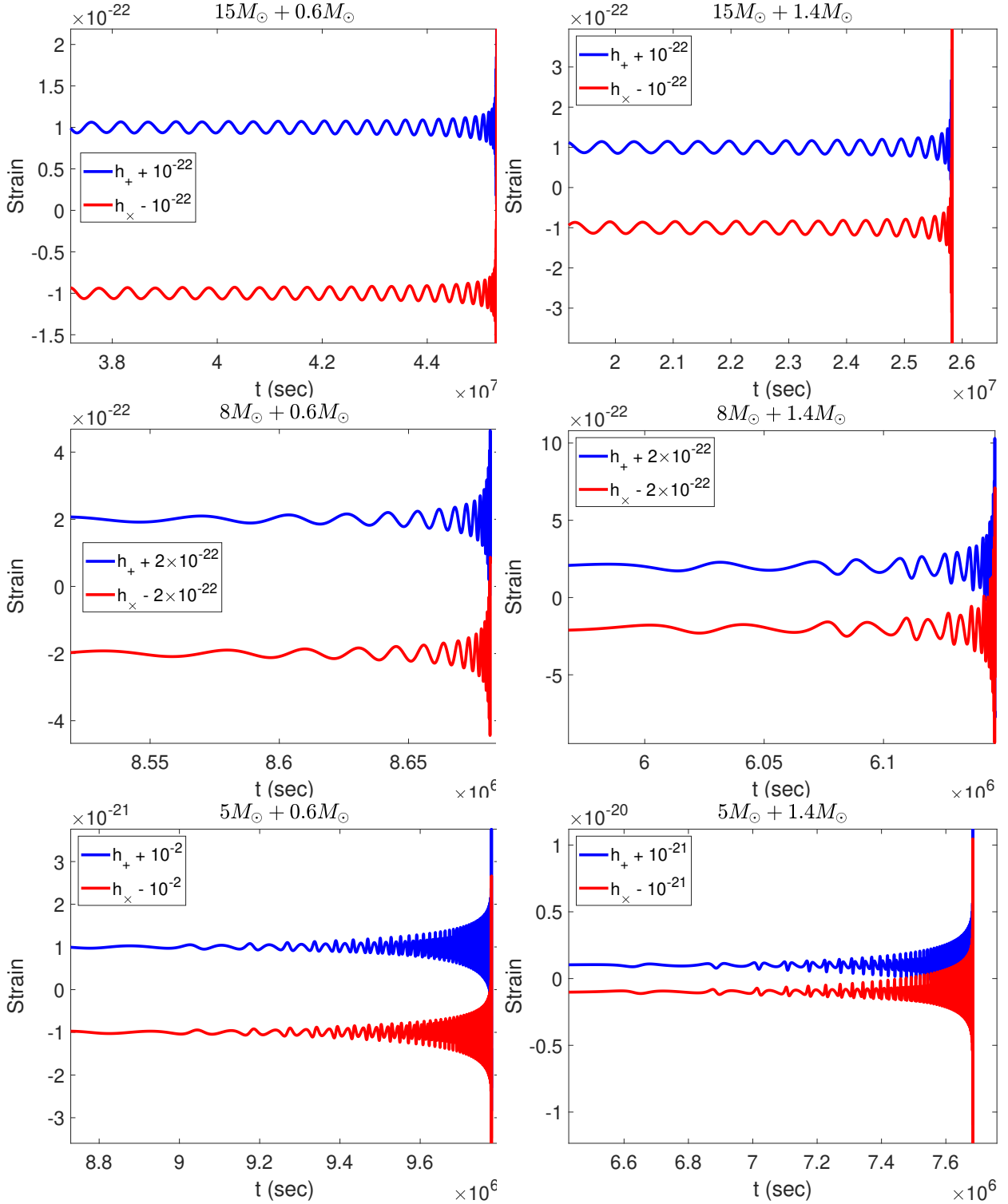


**Figure 2.** CEGWs (both polarizations), shown for the different combinations of COs and evolved star binaries, computed at a distance of 10kpc.

noise) then the SNR is given by (Moore et al. 2015)

$$\left(\frac{S}{N}\right)^2 = 4 \int_0^\infty \frac{|\tilde{h}(f)|^2}{S_n(f)} df = \int_0^\infty \frac{h_c^2(f)}{h_n^2(f)} df, \quad (8)$$

where  $\tilde{h}(f) = \int_{-\infty}^\infty e^{-2\pi i f t} h(t) dt$ . The characteristic strain is

$h_c(f) = 2f\tilde{h}(f)$ ; so, if  $h_n = \sqrt{fS_n(f)}$  signifies the sensitivity of the detector, the area between the characteristic strain and the sensitivity curve in logarithmic scale is the SNR. These are calculated using a discrete fast Fourier transform, applying a Tukey window (Abbott et al. 2016a) to alleviate spectral leakage.



The characteristic strains of the cases we considered here are presented at the top row of figure 3. SNRs for the three detectors: LISA, DECIGO and BBO, are presented in table 1. Note, that contrary to a gas-free GW in-spiral,  $h_c(f)$  is not proportional to a power of  $f$  – it is not a straight line in logarithmic scale.

## 5 EXTENDED ENVELOPES

As mentioned above, the models described here are simplified and neglect the evolution of the envelope itself due to the in-spiral. In reality, gravitational energy is deposited into the envelope by gas dynamical friction, which inflates the envelope and results in its partial or full unbinding (Ivanova et al. 2013). The in-spiral is therefore expected to occur in more extended density profiles than the initial one, and therefore the density close to the core should be lower. In this scenario the magnitude of the GDF force on the companion should be smaller, and the amount of time it spends very close to the core, emitting the strongest GWs, is increased. In other words, our SNR calculations serve as lower limits to the expected GW signatures for such CE-in-spirals, whilst being bounded by an upper limit – the expected signal from a gas-free in-spiral of two COs of similar masses (see the violet line in figure 3). As a simplified approach we gauge the magnitude of the extended-envelope effect using a simple, inflated envelope model, where we again integrate equation (1), but we now consider a density profile which is linearly dilated, with

$$\rho'(r) = \rho \left( \frac{r - R_{\text{core}}}{\lambda} + R_{\text{core}} \right) \lambda^{-3} \quad (9)$$

$$c'_s(r) = c_s \left( \frac{r - R_{\text{core}}}{\lambda} + R_{\text{core}} \right) \lambda^{-1/2}, \quad (10)$$

*etc.* A plausible scale-factor given results from hydrodynamical simulations of CE-evolution from the literature (Ivanova et al. 2013) is  $\lambda \approx 10$ ; the characteristic strains we find for the simplified extended envelopes are shown in the second row of figure 3 and the total SNRs are given in table 1.

As is evident from figure 3 and table 1 CE-in-spirals occurring in the Galaxy could potentially be observed by LISA, DECIGO or BBO, where the latter might even be sensitive to extra-Galactic sources up to distances of a few Mpc.

To test our semi-analytical calculations, we perform a hydrodynamical simulation for the case  $M + M_{\text{env}} = 8M_{\odot}$ ,  $m = 0.6M_{\odot}$ . Our simulation is run via the AMUSE framework (Portegies Zwart et al. 2009), which allows us to combine different type of codes. We use the same density profile for the  $8M_{\odot}$  red giant as above, and convert it to a 3-dimensional smoothed-particle-hydrodynamics (SPH) model with 250000 gas particles. The core is represented by a point mass (dark-matter particle) to avoid numerical issues and unnecessary calculation in this dense region, whose internal changes are irrelevant for our purposes. Since the MESA model is one-dimensional and is described by different evolution equations, we run a relaxation phase of the SPH model alone first, for about 1000 days, while we allow only small changes in the centre of mass velocity and position (a restriction which is lifted later on). After we have

a relaxed model, we use it to simulate the actual CE phase with the companion which is also modelled as a dark-matter particle. The simulation runs with the SPH code Gadget 2 (Springel 2005) until the core and the companion become closer than the smoothing radius. A more thorough explanation of the simulation is presented in Glanz & Perets (2018, 2020).

Figure 5 displays a comparison between the core-companion distance obtained from the SPH model, and with our approximation, taking  $\lambda = 11$ . Also shown is a plot of the characteristic strains from both cases. The comparison between our simplified approach and the SPH model is physically meaningful only down to the smoothing parameter, as the SPH model breaks down at lesser radii; in this range, the two agree, thereby justifying our model even at smaller distances which the SPH simulation cannot probe, too. Figure 4 displays the orbits in the two models.

## 6 SUMMARY

In this paper we explored gravitational-wave emission by the in-spiral of a compact object in an evolved common-envelope binary, leading to the final merger of the compact object with the stellar core of the evolved star. As we show the in-spirals differ significantly from gravitational-wave in-spirals of binary isolated compact objects; common-envelope in-spiral are dominated by a gas dynamical friction interaction with the envelope and not by dissipation from the gravitational-wave emission itself. Such an evolution changes the acceleration of the binary and yields gravitational-wave signatures with a unique frequency evolution. In particular such gravitational-wave sources could be potentially observable by next-generation gravitational-wave detectors such as LISA/DECIGO/BBO, and their unique frequency evolution could provide not only a smoking-gun signature for their origin, but also enable the use of gravitational-wave detectors for mapping the interiors of evolved stars, otherwise inaccessible through electromagnetic observations.

The common-envelope phase is also typically accompanied by explosive electromagnetic transients. The in-spiral itself might give rise to a luminous flare, possibly resembling stellar mergers such as V1309 Scorpii (Tylenda et al. 2011). The merger of a white dwarf (or neutron star) and the degenerate core might cause a thermonuclear explosion, potentially observable as peculiar luminous (sub-luminous) type II/Ib supernova (given the large amounts of hydrogen and helium in the envelopes). Finally, the in-spiral of a neutron star into the center of the evolved star may produce a Thorne-Żytkow object (Thorne & Żytkow 1977). Systems with heavier compact companions, such as black holes, may generate even stronger signals. Even though there is expected to be little accretion onto such small compact objects as we consider here (Glanz & Perets 2020), such accretion would generate gravitational waves at frequencies that are much higher than the characteristic ones for space-based detectors (Holgado et al. 2018; Holgado & Ricker 2019), leading to a possibility of observing the same process in many detectors at the same time.

Estimates of the rates of mergers of compact objects with degenerate cores of evolved stars leading to type Ia supernovæ suggest that they should occur at rates of

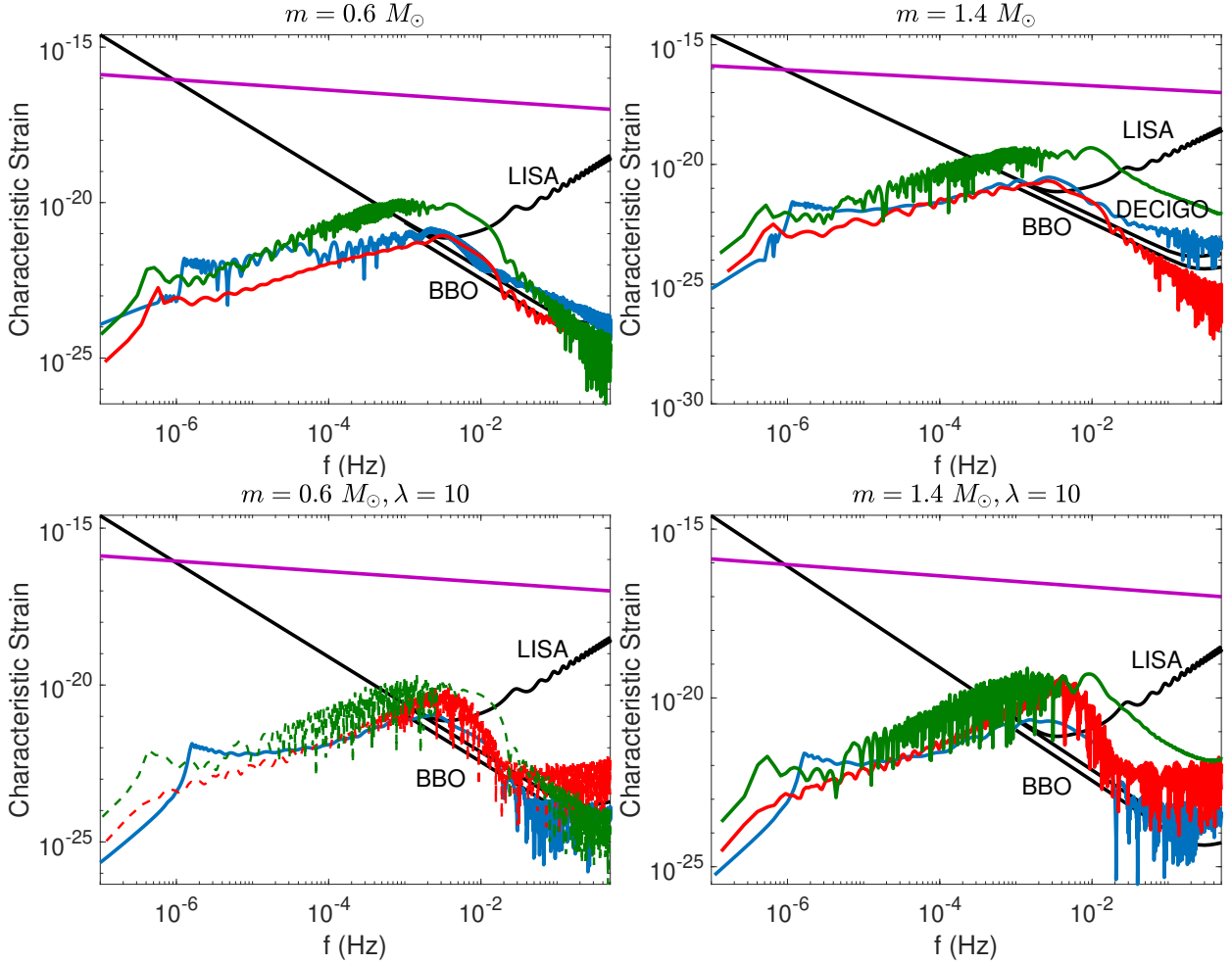


**Figure 3.** The characteristic strain of the in-spirals considered in this paper, together with the LISA, DECIGO and BBO sensitivity curves, in black. The blue curves correspond to  $M_{\text{tot}} = 15M_{\odot}$ , the red ones – to  $M_{\text{tot}} = 8M_{\odot}$ , and the green ones – to  $M_{\text{tot}} = 5M_{\odot}$ . As a reference, the violet curve shows a binary WD merger without any envelope, with  $m_1 = 1M_{\odot}$ ,  $m_2 = 0.6m_{\odot}$ . The left panels show the case of  $m = 0.6 M_{\odot}$ , and the right – a NS companion of  $1.4 M_{\odot}$ . The top row displays envelopes that remain compact, while the bottom row shows envelopes dilated by a factor of 10 (see text). All quantities are calculated at a distance  $D = 10$  kpc. The Fourier transforms are calculated by sampling the signal at a rate of 1 Hz. Sampling it at higher rates (necessary for DECIGO and BBO) should not decrease the SNRs.

**Table 1.** SNRs for the in-spirals discussed in the text for LISA/DECIGO/BBO.  $M_{\text{tot}}$  is defined as  $M + M_{\text{env}}$ . Cf. figure 3.

		$M_{\text{tot}} = 15 M_{\odot}$			$M_{\text{tot}} = 8 M_{\odot}$			$M_{\text{tot}} = 5 M_{\odot}$		
Envelope	$m (M_{\odot})$	LISA	DECIGO	BBO	LISA	DECIGO	BBO	LISA	DECIGO	BBO
Compact	0.6	0.57	1.3	3.4	0.42	0.25	0.63	4.6	1.43	3
Compact	1.4	1.3	2.83	7.5	0.88	0.26	0.53	20	94	230
Extended	0.6	0.48	0.33	0.9	2.3	6	19	5	1.5	3.2
Extended	1.4	1.1	1.1	3.2	11	20	63	21	77	200

10 – 100% of the observationally-inferred rates of type Ia SNe (Ilkov & Soker 2013; Tutukov et al. 1992); the rates of CEGW sources could be higher. Nazin & Postnov (1997) estimate a rate of  $0.002 \text{ yr}^{-1}$  for the formation of Thorne-Żytkow objects, based on Podsiadlowski et al. (1995), implying an overall rate of one CEGW event per a few centuries in our Galaxy. Although less likely to be observed by LISA given the expected Galactic rates, the DECIGO/BBO ob-

servatories would enable observing extra-Galactic CEGWs and potentially detect a few such events.

## ACKNOWLEDGMENTS

We wish to thank Andei P. Igoshev and Yael Raveh for helpful discussions. YBG and EG acknowledge support from the

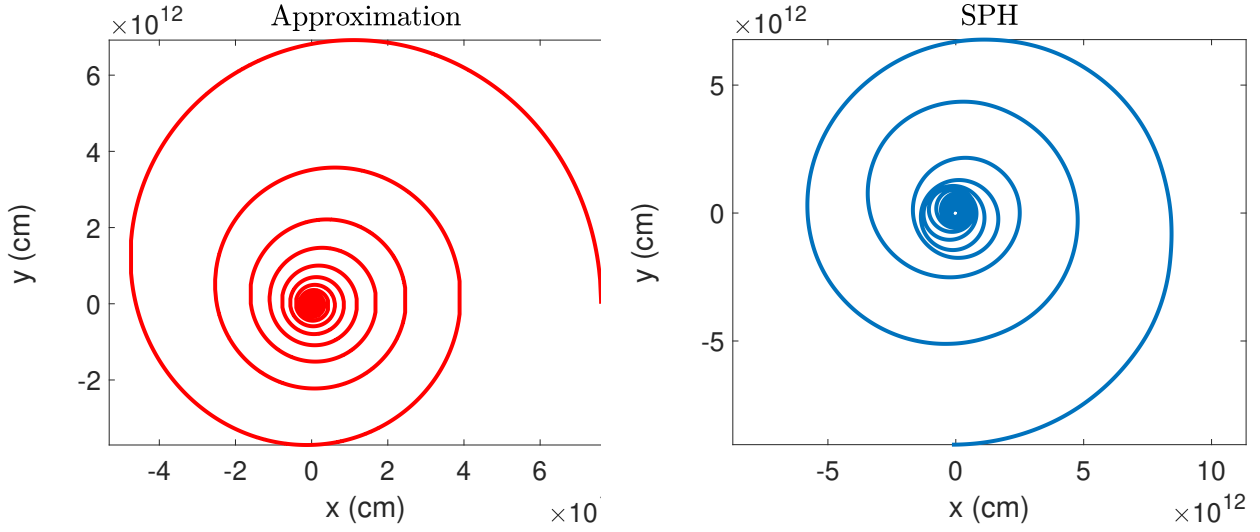


**Figure 4.** A comparison between the orbit – i.e. the separation between the companion and the core – in our approximation, taking  $\lambda = 11$ , and in the SPH model. Both cases have  $M + M_{\text{env}} = 8M_{\odot}$ ,  $m = 0.6M_{\odot}$ .

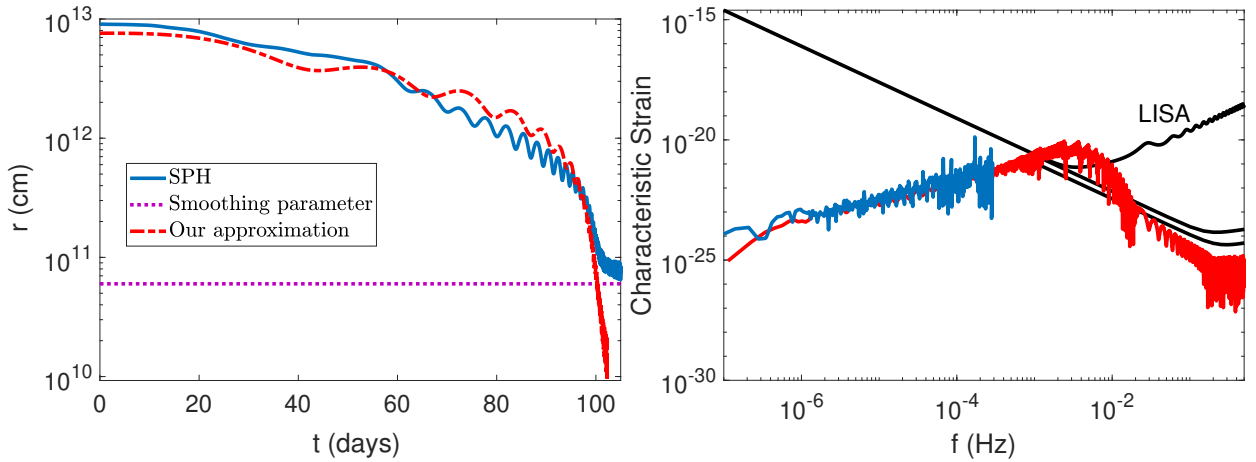


**Figure 5.** Left: the distances between the core and the companion, as computed from the SPH model (blue), and our approximation (red), for the case  $M + M_{\text{env}} = 8M_{\odot}$ ,  $m = 0.6M_{\odot}$ . The smoothing parameter is shown as a horizontal dashed line. Right: the characteristic strains of the gravitational-waves emitted by the system for both cases (the SPH model was sampled once per 0.02 days, hence its cut-off), observed from a distance of 10 kpc. Second row: the separation between the core companion and the core in the two models (our approximation – left; SPH – right).

Technion Jacobs scholarship; and VD acknowledges support by the Israel Science Foundation (grant no. 1395/16).

## REFERENCES

- Abbott B. P., et al., 2016a, *Phys. Rev. D*, **93**, 122003  
 Abbott B. P., et al., 2016b, *Physical Review Letters*, **116**, 061102  
 Abbott B. P., et al., 2018, arXiv e-prints,  
 Amaro-Seoane P., et al., 2017, arXiv e-prints, p. [arXiv:1702.00786](#)  
 Binney J., Tremaine S., 2008, *Galactic Dynamics: Second Edition*. Princeton University Press  
 Fedrow J. M., Ott C. D., Spherhake U., Blackman J., Haas R., Reisswig C., De Felice A., 2017, *Physical Review Letters*, **119**, 171103  
 Glanz H., Perets H. B., 2018, *MNRAS*, **478**, L12  
 Glanz H., Perets H. B., 2020, forthcoming  
 Grishin E., Perets H. B., 2015, *ApJ*, **811**, 54

- Holgado A. M., Ricker P. M., 2019, arXiv e-prints, p. [arXiv:1902.10716](#)  
 Holgado A. M., Ricker P. M., Huerta E. A., 2018, *The Astrophysical Journal*, **857**, 38  
 Ilkov M., Soker N., 2013, *MNRAS*, **428**, 579  
 Ivanova N., et al., 2013, *A&ARv*, **21**, 59  
 Kim H., Kim W.-T., 2007, *ApJ*, **665**, 432  
 Lincoln C. W., Will C. M., 1990, *Phys. Rev. D*, **42**, 1123  
 Maggiore M., 2008, *Gravitational Waves. Vol. 1: Theory and Experiments*. Oxford Master Series in Physics, Oxford University Press  
 Michaely E., Perets H. B., 2019, *MNRAS*, **484**, 4711  
 Moore C. J., Cole R. H., Berry C. P. L., 2015, *Classical and Quantum Gravity*, **32**, 015014  
 Nazin S. N., Postnov K. A., 1995, *A&A*, **303**, 789  
 Nazin S. N., Postnov K. A., 1997, *Astronomy Letters*, **23**, 139  
 Ostriker E. C., 1999, *ApJ*, **513**, 252  
 Pani P., 2015, *Phys. Rev. D*, **92**, 123530  
 Paxton B., Bildsten L., Dotter A., Herwig F., Lesaffre P., Timmes

- F., 2011, [ApJS](#), **192**, 3
- Paxton B., et al., 2013, [ApJS](#), **208**, 4
- Paxton B., et al., 2015, [ApJS](#), **220**, 15
- Podsiadlowski P., Cannon R. C., Rees M. J., 1995, [MNRAS](#), **274**, 485
- Portegies Zwart S., et al., 2009, [New Astron.](#), **14**, 369
- Springel V., 2005, [MNRAS](#), **364**, 1105
- Thorne K. S., Żytkow A. N., 1977, [ApJ](#), **212**, 832
- Tutukov A. V., Yungelson L. R., Iben Icko J., 1992, [ApJ](#), **386**, 197
- Tylenda R., et al., 2011, [A&A](#), **528**, A114

This paper has been typeset from a  $\text{\TeX}$ / $\text{\LaTeX}$  file prepared by the author.